SYNTHESIS OF Al-Sc MASTER ALLOYS THROUGH INDUCTION SUPPORTED METALLOTHERMY – PROCESS KINETICS AND TECHNICAL FEASIBILITY

*F. Brinkmann and B. Friedrich
Institute of Process Metallurgy and Metal Recycling (IME), RWTH Aachen University
Intzestr. 3, 52072 Aachen, Germany
*(*Corresponding author: fbrinkmann@metallurgie.rwth-aachen.de)*

ABSTRACT

The extraction of the critical metal Sc from oxidic or halogenous compounds is challenging due to the metal's high affinity to F, Cl or O and its physical properties, such as low density and high melting point, that pose high demands concerning processing techniques. We applied the principles of metallothermy, supported by induction heating in a vacuum induction furnace (VIM) in order to extract Al-Sc master alloys with Sc contents far above commercially viable materials. The reduction of ScF_3 with Al is found to be the most advantageous as it may be applied in conventional VIM with minor modifications, as the desired product is all-liquid with Sc contents > 12 Ma%. We designed a process scheme in which ScF_3 is charged semi-continuously to ensure maximum extraction efficiency. Besides the technical feasibility of the extraction process, we investigate the process kinetics and boundary conditions necessary for an efficient in-situ extraction of Al-Sc using advanced analysis methods. In the interface between the reactants, the formation of AlF_3 plays a crucial role as its evaporation accelerates the extraction dramatically.

KEYWORDS

Al-Sc, FactSage, Metallothermy, Scandium, Vacuum Induction Melting

INTRODUCTION

Sc is one of the most potent alloying elements for aluminum due to its strengthening effect and recrystallization inhibition, among others. Yet, its low global supply (2019: 15 – 20 tons per year) (Gambogi, 2020) impedes major application fields, e.g. in aerospace. Hence, efficient processing schemes are desired as the objective is to reduce costs and extract Sc at high yields.
As Sc alloying as pure substance in conventional gas-powered Al furnaces is subjected to elevated losses due to oxidation, master alloys are a superior option. Solubility calculations via FactSage (Bale et al., 2016) determine the scope that Sc concentrations may be varied at certain Al temperatures (Table 1). In fact, commercial Al-Sc master alloys at 2 Ma% Sc are far below values that are theoretically achievable.

Table 1. Solubility limits of Sc in liquid Al at various temperatures

Temperature in °C	Sc content in Ma%
1000	8.47
1100	13.43
1200	19.71
1300	29.29
1400	39.51

The approach for most experimental research is to dissolve ScF_3 in a suitable salt slag and to induce the reduction by bringing it in contact with Al (Xu et al., 2012). The strong advantage of this technology is the high Sc conversion yield (up to 91 % for Al-Sc 2 %) as well as the prevention of harmful off-gases. On the other hand, only low Sc concentrations may be incorporated in the Al melt and the resulting slag residue phase has little economic value. By using pure ScF_3 and Al as input material, higher Sc contents in the Al matrix are achievable. Data in the literature indicate that the maximum Sc content is governed determined by the process temperature – at a maximum temperature of 1040 °C, Sc content reached 10 % (Mukhachov, Kharitonova, & Skipochka, 2016). However, processing with this system leads to the formation of fluoridic gases, mainly AlF and AlF_3. A thorough analysis of the sublimates is given by Sokolova, Pirozhenko and Makhov (2015). Alternative approaches revolve around the simultaneous co-reduction of Al_2O_3 and ScF_3 with Ca, yielding not only a Sc-rich Al phase, but also a liquid slag phase (Brinkmann, Mazurek, & Friedrich, 2019).
Used refractory materials are usually graphite (Xu et al., 2012; Mukhachov, Kharitonova, & Skipochka, 2016) or tantalum (Spedding, Daane, Wakefield & Dennison, 1960; Harata, Nakamura, Yakushiji, & Okabe, 2008; Daane & Spedding, 1953; Gschneidner, 1978). MgO refractory material was used at the beginning of the research on Sc reduction (Fischer, Brünger & Grieneisen, 1937). Furnaces used for the reduction step are induction furnaces in open atmosphere (Xu et al., 2012), a retort type reactor (Mukhachov et al., 2016) and resistance heating furnaces (Daane & Spedding, 1953; Harata et al., 2008; Sokolova et al., 2015).
Hydrofluoric acid is used for ScF_3 synthesis in the classical approach. Since the handling of HF is implicating safety issues and an additional processing step is involved, the Sc extraction from Sc_2O_3 is desired. Thus, metallothermic reduction of the oxide is thermochemically unfeasible for pure substances on a technological basis. Therefore, different approaches are described in the literature that mostly comprise in-situ conversion of the oxide to fluoride. (Harata et al., 2008) used a mixture of Al and Ca as reducing agent and produced an alloy with roughly 9 wt.-% Sc in the Al matrix, indicating a complete conversion of the oxide into the metallic form. Other researchers state that it is sufficient to skip the master alloy production step by directly introducing Sc_2O_3 to the aluminum melt, giving the desired Sc concentration. (Røyset & Ryum, 2005)

METALLOTHERMY

Metallothermic reduction is a particular case of a self-propagating high-temperature synthesis (SHS). Here, a metal or alloy is used as reducing agent for the non-metallic precursor substance, most commonly in the form of oxides or halides. Thus, reaction enthalpies are the crucial factor for the self-propagating nature of these reactions, if the activation energy is overcome prior by a sufficient methods.
The main reaction governing the investigated process is given in equation 1.

$$<ScF_3> + 4\ (Al) \rightarrow [Al_3Sc]_{Al} + <AlF_3> \quad (1)$$

If surplus Al is available, AlF_3 may further react with Al to form gaseous AlF (equation 2), resulting in the overall reaction expressed in equation 3.

$$<AlF_3> + 2\ (Al) \rightarrow 3\ \{AlF\} \quad (2)$$
$$<ScF_3> + 6\ (Al) \rightarrow [Al_3Sc]_{Al} + 3\ \{AlF\} \quad (3)$$

Thermochemistry

To compute the thermochemical characteristics of the system, the software tool FactSage™ 7.3 (Bale et al., 2016) is used. In particular, the data bases applied for the following calculations are FactPS, FTlite and FThall. The modules “Equilib” and “Reaction” are chosen to simulate the following system behaviors.

The concept of adiabatic temperature is used to estimate the heat balance of a metallothermic reduction as heat capacities and/or enthalpy of fusion among others are offset against reaction enthalpies. For a simplistic first approach, ScF_3 to Al at the molar ratio of equation 3 is assumed to observe the dependency of the adiabatic temperature on pressure. Note that the initial temperature chosen is always the given temperature of the Al melt, while ScF_3 is added at 25 °C (Figure 1).

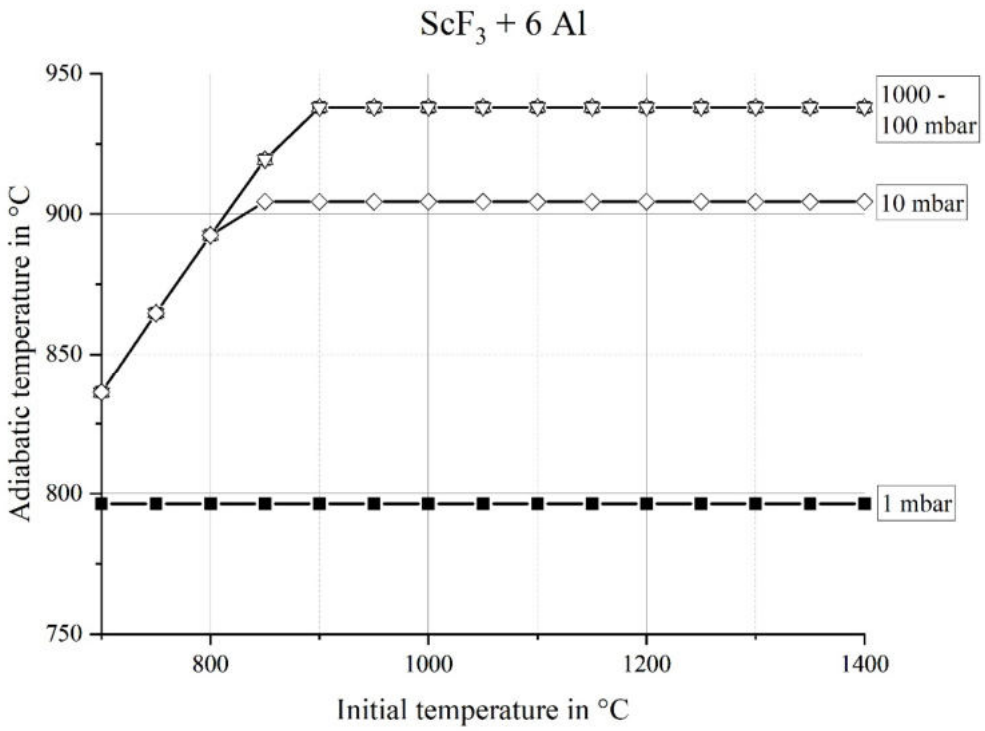

Figure 1. Adiabatic temperatures of the aluminothermic ScF_3 extraction at various pressures

In the scenario described in this paper, the adiabatic temperature eventually falls below the starting temperature, indicating the endothermic behavior of the overall extraction (see Figure 1). However, low pressures seem to be favorable, due to the constant adiabatic temperature that indicates a full consumption of the initial energy supplied by the elevated initial temperature. Given this observation, a constant energy supply by an external heat source is mandatory in order to ensure a complete reaction.

The changes the system undergoes are strongly depending on temperature and pressure. To track the reaction mechanisms during the curse of a reaction, equilibrium calculations were conducted. In order to model the system in accordance with the existing boundary conditions of the furnace type used, the following assumptions are made:

- Virtually open system: any material reporting to the gas phase is removed from the system
- Reaction starts above the liquidus temperature of the reducing agent Al: 700 °C
- Sublimation pressure of ScF_3 as restricting upper temperature threshold: 1400 °C
- Products may be assumed as in their liquid composition: no segregation during tapping
- Temperatures are not decreasing at any times
- Pressures remain constant throughout the course of the reaction: 1 mbar and 1000 mbar

Thus, stepwise equilibrium calculations are considered, for which the previous products are recirculated. Starting at 700 °C with 250 g of an all-liquid Al phase, 6 g ScF_3 are added to the melt, coupled with a

(forced) temperature increase of 50 °C. Subsequently, the calculation is repeated with the reacted product, from which the gas phase (if occurring) is discarded. The process is repeated 15-fold, up to 1400 °C and 90 g of ScF_3 input.

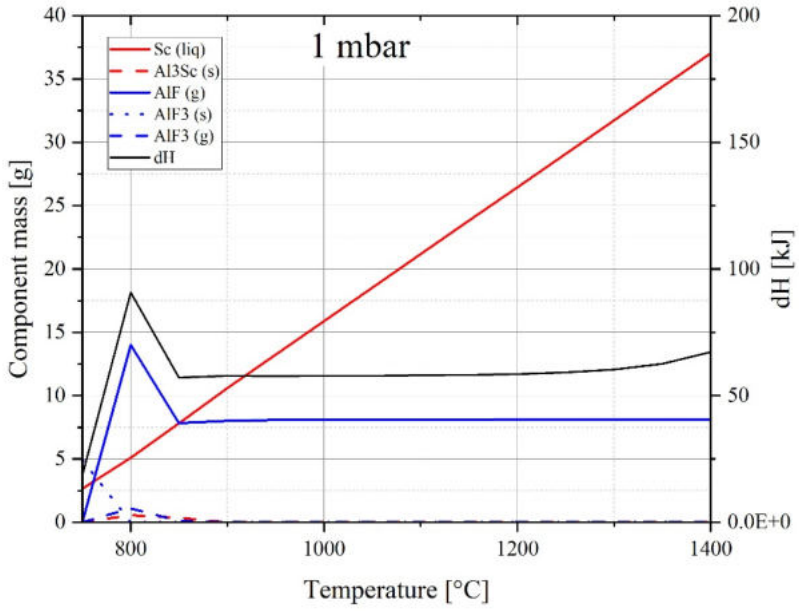

Figure 2. Equilibrium phase distribution and enthalpy change at 1 mbar

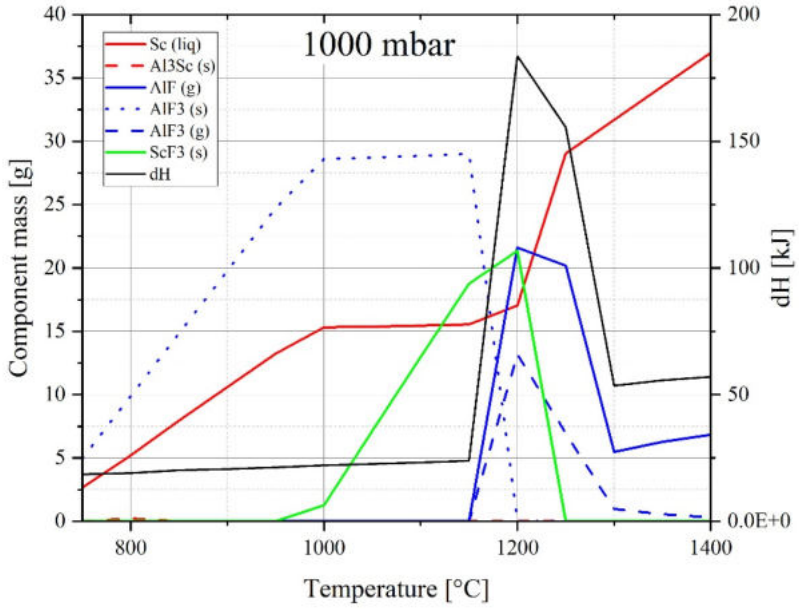

Figure 3. Equilibrium phase distribution and enthalpy change at 1000 mbar

Processing under vacuum conditions (1 mbar, Figure 2) is found to be more constant relative to atmospheric pressure levels (1000 mbar, Figure 3). Hence, following a reaction regime that produces mostly AlF_3(s) as by-product to Sc dissolved in Al, AlF becomes the principle gas component at temperatures exceeding 800 °C. The conversion remains constant, as derived from the adiabatic energy demand of the reaction (dH). Reaction conditions differ strongly, however, if pressures are elevated. Here, AlF_3(s) is synthesized as by-product until the temperature is increased to 950 °C with similar extraction rates at relatively lower enthalpy requirements due to the absence of an emerging gas phase. As the fluoridic by-product is not constantly removed in this scenario, ScF_3(s) eventually remains unreacted. It is due to the evolving AlF(g) that the reaction may resume at temperatures around 1200 °C, also indicated by the vast enthalpy requirement of the reduction within this temperature range. Note that not only AlF(g) is formed, but also AlF_3(g) is reporting to the gas phase. At the upper limit of the investigated temperature range, extracted Sc is at the same mass regardless of the working pressure.

The simulation at two different pressures highlight the extraction's strong dependency on this parameter. In total, the process is governed by the interaction of AlF_3 and Al (equation 2).

Kinetics

Two crucial kinetic barriers to the extraction system are identified. First, heat transport from the melt to ScF_3 needs to be sufficiently high to ensure a constantly ongoing reaction. Second, any solid phase forming in the interface between the reactants significantly reduces reaction rates as diffusion problems need to be considered. Here, we focus on the heat transfer between ScF_3 and Al.

As induction powered melt agitation is turbulent, a heat transfer by convection is the major energy transport phenomenon. In terms of dimensionless quantities, Nusselt number (Nu) is defined as

$$Nu = \alpha \cdot L \cdot \lambda^{-1} \tag{4}$$

In the case of forced convections, it is described by Reynolds number (Re) and Prandtl number (Pr). In our scenario, the characteristic length of the system is the diameter of the ScF_3 tabloid with 40 mm. Flow velocities are difficult to derive due to the unbalanced flow profile and various side effects. Experimental data is reported by Vivès and Ricou (1985) for a molten Al bath stirred by induction in a 1100/2000 Hz furnace. Measured velocities are in the range of 0.1 ms^{-1}; this value was thus chosen for the estimation of Re number. The density and thermal conductivity of pure Al is derived from the work of Leitner, Leitner, Schmon, Aziz and Pottlacher (2017). Kinematic viscosity data is taken from Konstantinova, Kurochkin and Popel (2011) in the range from 700 – 1100 °C; Argyropoulos, Mikrovas and Doutre (2001) state a correlation for Nu, Re and Pr in a single-phase forced convection flow in liquid Al (Equation 5).

$$\overline{Nu}_D = 2 + 10^{2.811} \cdot \overline{Re}_D^{0.585} \cdot \overline{Pr}_D^{2.386} \tag{5}$$
$$5162 \leq Re_D \leq 21{,}273,\ Pr \approx 0.014$$

Hence, dimensionless quantities are calculated (Table 2). It is assumed that equation 5 is valid for all Pr numbers.

Table 2. Dimensionless quantities at various temperatures and heat transfer coefficient

Temperature in K	Flow velocity in ms^{-1}			α in $Wm^{-2}K^{-1}$
	Re	Pr	Nu	
973.15	***8016.0***	***0.0154***	***7.876***	***17881***
1073.15	***9732.4***	***0.0120***	***5.664***	***13370***
1173.15	***10810.8***	***0.0103***	***4.716***	***11510***
1273.15	***11904.8***	***0.0090***	***4.072***	***10217***
1373.15	***12903.2***	***0.0049***	***2.501***	***6421***

Subsequently, the projected reaction times are calculated in the temperature range between 850 and 1100 °C. By considering the adiabatic temperatures given in Figure 1, the temperature gradient between the reaction zone and the liquid aluminium is assumed to be the current melt temperature (T_m) subtracted by the adiabatic temperature (T_a). Note that the reaction is exothermic up to 800 °C; here, only the endothermic case is regarded. Area A is given by the tabloid's surface. Thus, the heat flow Q is calculated by Equation 6. With this, the required time for a complete reduction of a tabloid of 6 g is determined by the enthalpy requirement of the reduction at given temperature, divided by the corresponding heat flow (Figure 4).

$$Q = \alpha \cdot A \cdot (T_m - T_a) \tag{6}$$

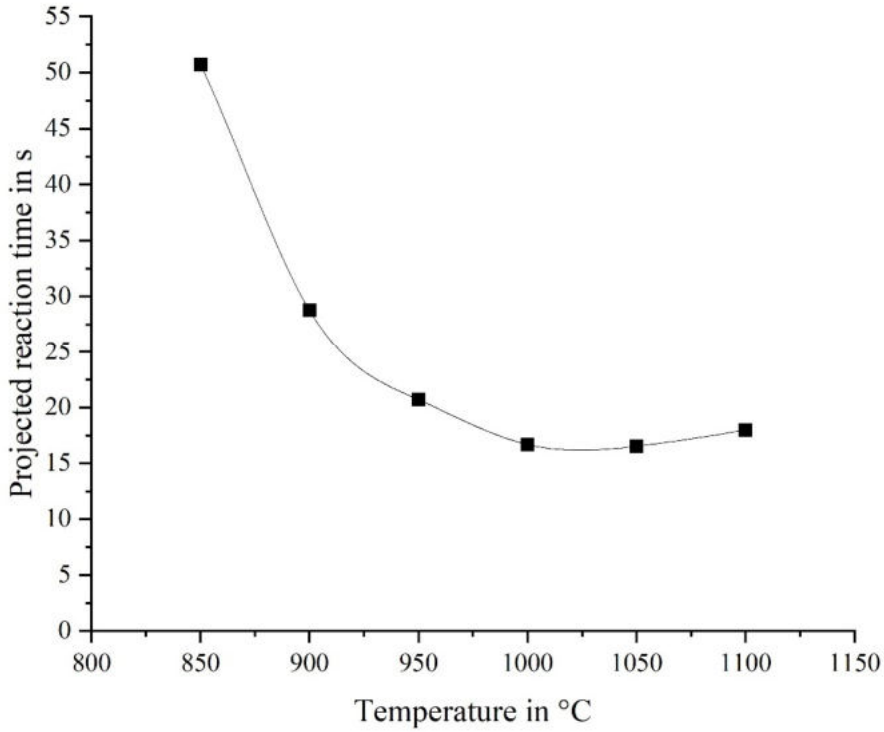

Figure 4. Projected reaction times at 1 mbar

As reaction times are decreasing with increasing melt temperature, it is beneficial to initiate the feeding of individual ScF_3 compacts at 950 °C and above.

EXPERIMENTAL

The experiments are conducted in cold-walled 10 kHz vacuum induction furnaces. Here, an alternating current (AC) runs through a copper coil, which therefore generates a magnetic field. The feed material inside is thus subjected to induced voltages, whereby eddy currents are generated if the material is electrically conductive. These currents gradually heat the material, in which is current density is decreasing towards the inside at a rate determined by the material's electrical properties and the applied frequency. In the molten state, the material is also exposed to strong bath agitation which results in strong turbulent mass flows and bath Meniscus. The copper coil is situated, among other installations, in a closed vacuum chamber ("cold-

wall" design) that may be evacuated and operated under vacuum conditions, or else under a protective gas atmosphere.
For orientational purposes, initial experiments are performed in a 160 ml crucible furnace with a maximum inductive power of 4 kW. Gas atmosphere within the system is adjusted by mechanical vacuum pumps for evacuation to pressures as low as $6 \cdot 10^{-2}$ mbar after flushing twice with Ar. Final pressures may be adjusted by an Ar gas inlet to 600 mbar. The copper coil, in which a graphite crucible is acting as susceptor inside a ZrO_2 packed bed (Figure 4), is not tilted during the experiment. Temperatures are constantly monitored by two thermocouples, which are embedded in protection tubes made of Al_2O_3. As material, Al fines (99.7 % purity) are used, as well as ScF_3 powder with 99.58 % purity. All experiments were carried out with 10 g ScF_3 and the corresponding mass of Al to fully reduce ScF_3 (1200 °C: 45.2 g, 1400 °C: 15.7 g). Prior to the experiment, the material is mixed and placed inside the crucible.

Figure 4. 160 ml graphite crucible with charged feed material

A larger vacuum induction furnace is used for the pilot experiments (max. 40 kW, max. melt volume 2.5 l). Oxidic crucibles are used (spinell type, $Al_2O_3 \cdot MgO$) It is equipped with an interlock that enables the operation of auxiliary tools for re-charging, additional temperature measurements and mechanical manipulation of the melt surface. Furthermore, a tiltable condenser unit is applied to capture any volatile components by condensation on the water-cooled condenser surface. A BN-coated bottom-cooled steel mould (cylindrical, Ø 40 mm, 68 mm height) is situated on a rotary copper disk to accommodate cast material.

Figure 5. Vacuum induction furnace after trial with AlF_3-covered copper condenser

Mechanically pressed ScF_3 tabloids of 6 g (40 mm diameter) are charged in discrete time steps between 10 – 20 min, resulting in a theoretical conversion rate of 0.3 – 0.6 g/min ScF_3. 4 tabloids are initially charged together with Al granules (250 g); subsequently, ScF_3 is charged according to the projected conversion plan. Temperature increases corresponds to the liquidus temperature of the Al-Sc phase that is intended to be overheated by 50 °C during the trial in order to prevent unwanted solidification; its magnitude is continuously tracked by a type B thermocouple, enclosed within a Y_2O_3-coated Al_2O_3 protection tube. Pressures are adjusted to 3 mbar prior to the charging of the first tabloid; subsequently, the pressure is adjusted to higher values if the reaction and gas formation become exceedingly violent and cause spillages. In between feeding steps, the copper condenser is placed upon the crucible (Figure 5), in order to collect condensed AlF_3. After feeding is complete, the coil is tilted to tap the metal into a cylindrical steel mould with BN-coating that is indirectly bottom-cooled (Figure 5**Fehler! Verweisquelle konnte nicht gefunden werden.**).

RESULTS

In lab scale, the Sc content in the metal phase reached 27.4 Ma%, with a conversion yield of 74.1 % in the sixth trial. The average Sc content at 1400 °C is 23.5 Ma% and therefore higher than in commercial Al-Sc master alloys with conventional 2 Ma%. Higher temperatures with lower holding times are influencing the conversion rate of Sc positively. Note that a temperature threshold exists that amplifies the conversion yield and Sc content to admissible values. The condensed phase from the crucible lid was analyzed via SEM-EDS and indicates strongly that AlF_3 is the major compound present in this phase with only minor Sc contaminations.

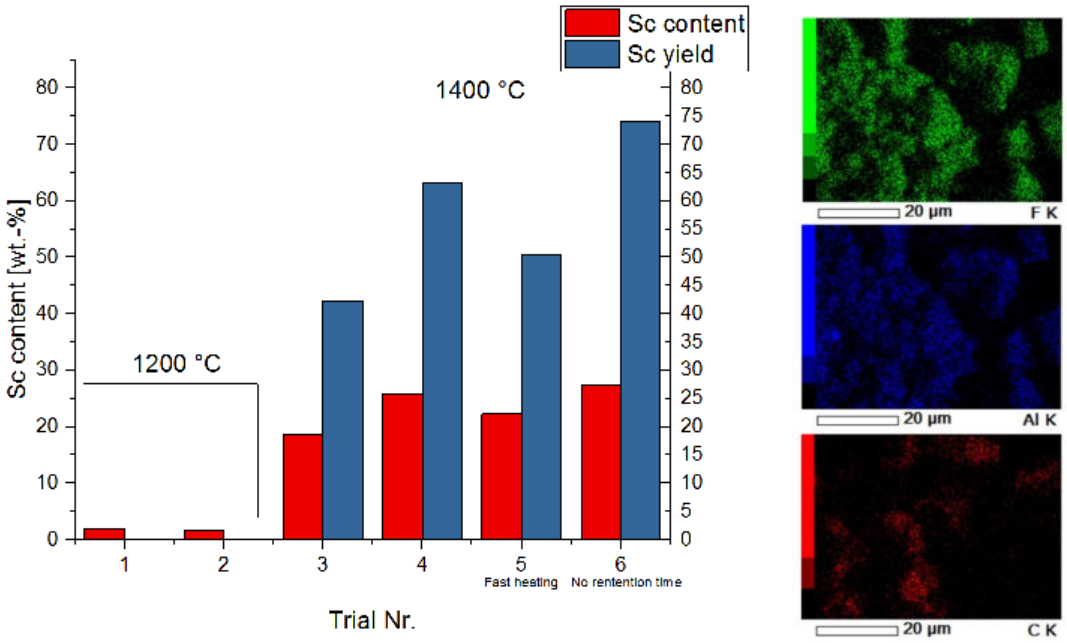

Figure 6. Left: Sc yield and concentrations of the lab scale experiments. Right: EDS-SEM condensate map of F, Al and C

The temperature and pressure profile of one pilot scale experiment is depicted in Figure 7. Along with the charging of the first tabloid, Al temperature begins to fluctuate heavily, demonstrating the unsteady endothermic behavior of the reduction process. 12 tabloids (total: 72 g ScF_3) were charged, corresponding to a theoretical Sc concentration of 16.48 Ma% at 100 % yield. The total time of the process was 216 min; the feeding time frame extended to 168 min, which results in a feeding rate of 0.43 $g \cdot min^{-1}$.

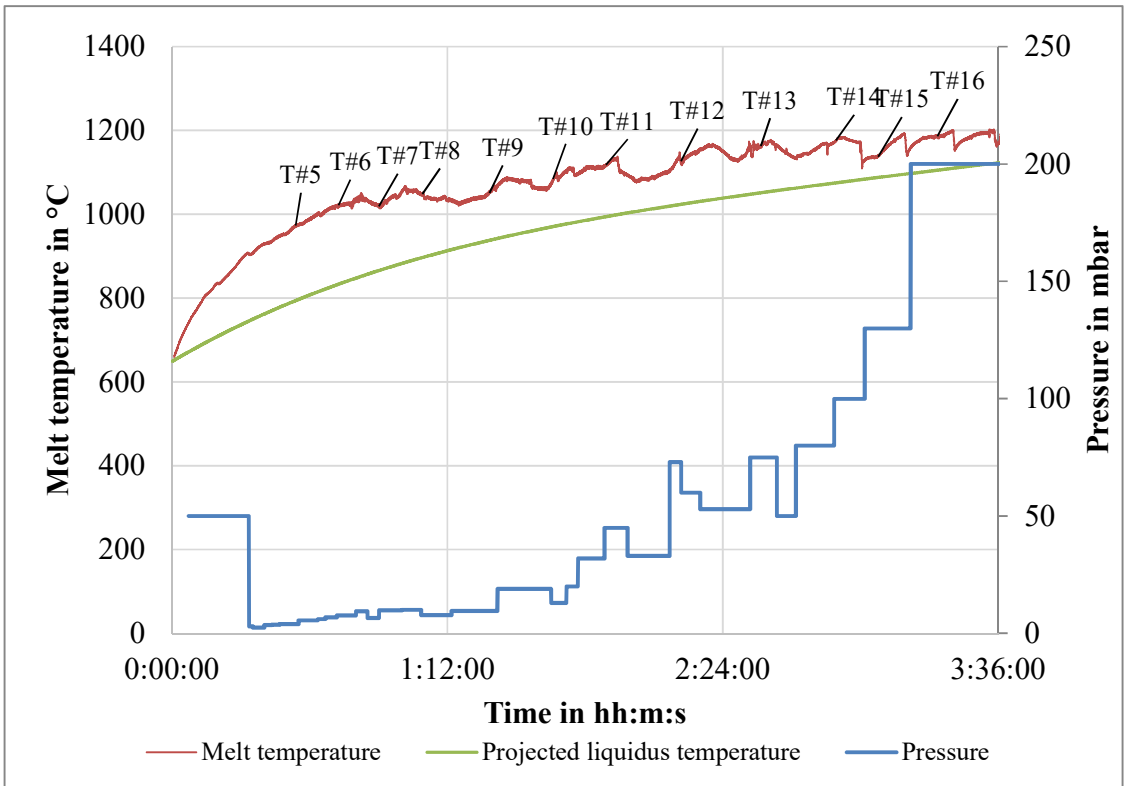

Figure 7. Temperature and pressure profile of an exemplary extraction experiment with projected liquidus temperatures

The cast specimen is cut in the center and mechanically prepared for micro XRF analysis. Each pixel is analyzed for 200 ms, whereas spots that were considered as points of interest (POI) are analyzed for 10 s. The map for the experiment described above is shown in Figure 8. The numerical values for particular POI are listed in Table 5. With an expected Sc concentration of 16.48 Ma%, the analyzed mean value is at 12.03 Ma%.

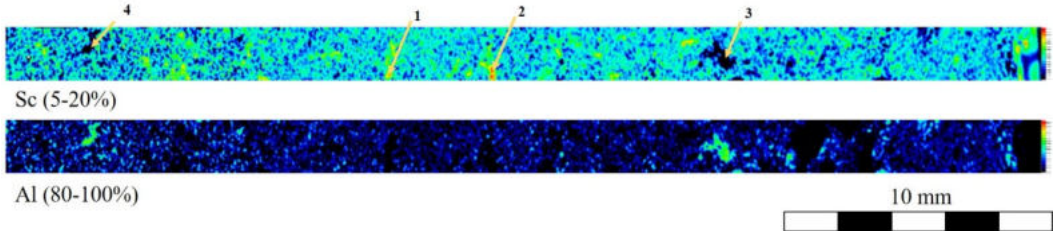

Figure 8. Sc and Al elemental distribution maps in the central radial plane of the cast specimen.

Table 5. micro XRF analysis of the cast sample

POI	Al in Ma%	Sc in Ma%	Si in Ma%
1	***85.53***	***9.58***	***3.85***
2	***74.41***	***20.81***	***3.04***

3	***91.36***	***1.78***	***5.89***
4	***83.94***	***12.28***	***3.10***

DISCUSSION

Sc concentrations exceeding commercially available Al-Sc master alloys are synthesized by the aluminothermic approach presented in this paper. In lab scale experiments, Sc yields up to 74 % are achieved, with 27 Ma% Sc in an Al matrix. The small scale trials also indicate a strong dependence on the temperature, as 1200 °C only accounted for minor Sc conversions. Al and F are found to be the major constituents of the condensed phase found on the lit of the crucible, supporting the theory of AlF/AlF_3 evaporation during the process. For the pilot scale, a profound understanding of the kinetic aspects of the process are sought, as the experimental setup is related to the technical feasibility in larger, semi-continuous scales with reusable crucibles. Just as the kinetic model shows, the heat transfer provided by the Al melt to deliver the energy needed for the underlying endothermic reaction is sufficient to ensure a reasonably fast reaction rate. Low pressures in the range of 1 mbar are necessary to promote the formation of gaseous AlF rather than solid AlF_3 in order to remove any material building up within the reaction zone. However, the required pressure levels cannot be maintained during the extraction, due to heavy material spillage as low pressures promote gas formation. Hence, process times rise sharply, as the experiment presented lasted over 4 hours. The temperature fluctuates strongly as soon as the charging of ScF_3 tabloids is initiated. Nevertheless, the cast alloy exhibits a heterogeneous microstructure with 12.03 Ma% Sc on average; segregation effects due to the initial precipitation of Al_3Sc in the analyzed part are found as the relative standard deviation of Sc is at 36.54 %.

CONCLUSION

The observed temperature fluctuations are accounted to the heat balance of the endothermic reaction, as temperature decreases are mainly occurring after the charging of an individual ScF_3 tabloid. We suggest a process mechanism that relies mostly on the removal of the Al-F side product formed during the extraction of Sc (Figure 9). As the gaseous species AlF is favored over the subliming compound AlF_3, low system pressures in the range of 1 mbar need to be ensured. However, with the setup used, material spillage due to gas formation cannot be obviated at 1 mbar, resulting in higher operating pressures and thus larger process times. We suggest that AlF_3 is thus hindering material transfer in the reaction zone, as Al and Al_3Sc permeation is decelerated.

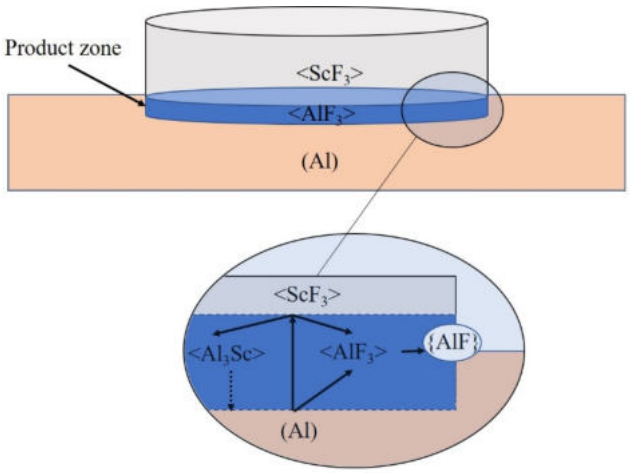

Figure 9. Proposed reaction mechanism for the aluminothermic ScF_3 extraction

Heat transfer does not prove to be the rate limiting step, as theoretically derived process times are largely outreached by the actual process times. Thus, induction support is a valid approach to ScF_3 reduction with Al. However, design changes must be realized to safely operate the process under lower pressures to accelerate reaction times.

ACKNOWLEDGEMENTS

This research was funded by the European Union's Horizon 2020 research and innovation program under the Grant Agreement No. 730105-SCALE. The authors would like to thank Markus Lenz from the University of Applied Sciences and Arts Northwestern Switzerland, for the micro XRF analyses.

REFERENCES

Argyropoulos, S. A., Mikrovas, A. C., & Doutre, D. A. (2001). Dimensionless correlations for forced convection in liquid metals: Part I. Single-phase flow. *Metallurgical and Materials Transactions B: Process Metallurgy and Materials Processing Science*, *32*(2), 239–246. https://doi.org/10.1007/s11663-001-0047-1

Bale, C. W., Bélisle, E., Chartrand, P., Decterov, S. A., Eriksson, G., Gheribi, A. E., … Van Ende, M. A. (2016). FactSage thermochemical software and databases, 2010-2016. *Calphad: Computer Coupling of Phase Diagrams and Thermochemistry*, *54*, 35–53. https://doi.org/10.1016/j.calphad.2016.05.002

Brinkmann, F., Mazurek, C., & Friedrich, B. (2019). Metallothermic Al-Sc co-reduction by vacuum induction melting using Ca. *Metals*, *9*(11). https://doi.org/10.3390/met9111223

Daane, A. H., & Spedding, F. H. (1953). Preparation of Yttrium and Some Heavy Rare Earth Metals. *Journal of the Electrochemical Society*, *100*(10), 442–444. https://doi.org/10.1149/1.2780875

Fischer, Werner; Brünger, Karl; Grieneisen, H. (1937). Über das metallische Scandium. *Zeitschrift Fur Anorganische Und Allgemeine Chemie*, *231*, 54–62.

Gambogi, J. (2020). Scandium. In *Mineral Commodity Summary*. https://doi.org/10.3133/70170140
Gschneidner, K. A. (1978). *Handbook on the Physics and Chemistry of Rare Earths*.

Harata, M., Nakamura, T., Yakushiji, H., & Okabe, T. H. (2008). Production of scandium and Al-Sc alloy by metallothermic reduction. *Transactions of the Institutions of Mining and Metallurgy, Section C: Mineral Processing and Extractive Metallurgy*, *117*(2), 95–99. https://doi.org/10.1179/174328508X290876

Konstantinova, N., Kurochkin, A., & Popel, P. (2011). Viscosity and volume properties of the Al-Cu melts. *EPJ Web of Conferences*, *15*. https://doi.org/10.1051/epjconf/20111501024

Leitner, M., Leitner, T., Schmon, A., Aziz, K., & Pottlacher, G. (2017). Thermophysical Properties of Liquid Aluminum. *Metallurgical and Materials Transactions A: Physical Metallurgy and Materials Science*, *48*(6), 1–10. https://doi.org/10.1007/s11661-017-4053-6

Mukhachov, A. P., Kharitonova, E. A., & Skipochka, D. G. (2016). Scandium and its alloys with aluminum. *Problems of Atomic Science and Technology*, *101*(1), 45–50.

Røyset, J., & Ryum, N. (2005). Scandium in aluminium alloys. *International Materials Reviews*, *50*(1), 19–44. https://doi.org/10.1179/174328005X14311

Sokolova, Y. V., Pirozhenko, K. Y., & Makhov, S. V. (2015). Concentration of scandium during processing the sublimate of production of the aluminum-scandium master alloy. *Russian Journal of Non-Ferrous Metals*, *56*(1), 10–14. https://doi.org/10.3103/S1067821215010186

Spedding, F. H.; Daane, A. H.; Wakefield, G.; Dennison, D. H. (1960). Preparation and Properties of High Purity Scandium Metal. *Transactions of the Metallurgical Society of AIME*, *218*, 608–611.

Vivès, C., & Ricou, R. (1985). Fluid flow phenomena in a single phase coreless induction furnace. *Metallurgical Transactions B*, *16*(2), 227–235. https://doi.org/10.1007/BF02679714

Xu, C., Liu, X., Ma, F., Wang, Z., Wang, W., & Ma, C. (2012). Preparation of Al-Sc Master Alloy by Aluminothermic Reaction with Special Molten Salt. *13th International Conference on Aluminum Alloys (ICAA13)*, 195–200.